ISSN 0020-4412, Instruments and Experimental Techniques, 2022, Vol. 65, No. 3, pp. 474–481. © Pleiades Publishing, Ltd., 2022.
Russian Text © The Author(s), 2022, published in Pribory i Tekhnika Eksperimenta, 2022, No. 3, pp. 100–107.

GENERAL EXPERIMENTAL TECHNIQUE

A Kicker Magnet for Beam Extraction from the Booster into the Booster–Nuclotron Beamline of the NICA Complex

O. V. Anchugov[a], D. A. Shvedov[a,*], V. A. Kiselev[a], A. N. Zhuravlev[a], S. V. Sinyatkin[a], D. I. Bazhutov[a], A. V. Tuzikov[b], A. A. Fateev[b], and A. S. Petukhov[b]

[a] *Budker Institute of Nuclear Physics, Siberian Branch, Russian Academy of Sciences, Novosibirsk, 630090 Russia*

[b] *Joint Institute for Nuclear Research (JINR), Dubna, Moscow oblast, 141980 Russia*

**e-mail: D.A.Shvedov@inp.nsk.su, shvedda@mail.ru*

Received December 29, 2021; revised February 2, 2022; accepted February 3, 2022

Abstract—A kicker magnet has been developed for the NICA accelerator complex at the JINR (Dubna) for ejecting ions into the beamline that connects the Booster and Nuclotron synchrotrons. An asymmetric design of the magnet without a ferromagnetic core is used to obtain the required magnetic field of 0.17–0.18 T in the region of the extracted beam. A power-supply system is proposed for the kicker magnet; it is based on two generators with different polarities, which are connected from opposite ends. This kicker magnet has made it possible to successfully extract He and Fe ions from the NICA Booster in accordance with the specified parameters.

DOI: 10.1134/S0020441222040029

1. "IRONLESS" KICKER MAGNETS

1.1. Symmetric Scheme of Field Formation

Unlike commonly used ferrite kickers with a ceramic vacuum chamber [1], the deflecting magnetic field is formed in kicker magnets without ferromagnetic cores by current-carrying conductors and conductive shields [2]. One of the simplest variants of such a magnet is shown in Fig. 1, which convincingly illustrates the characteristic situation for an ion booster when an injected beam fills the entire acceptance. The beam is then adiabatically attenuated during the acceleration process and becomes significantly smaller in size by the time

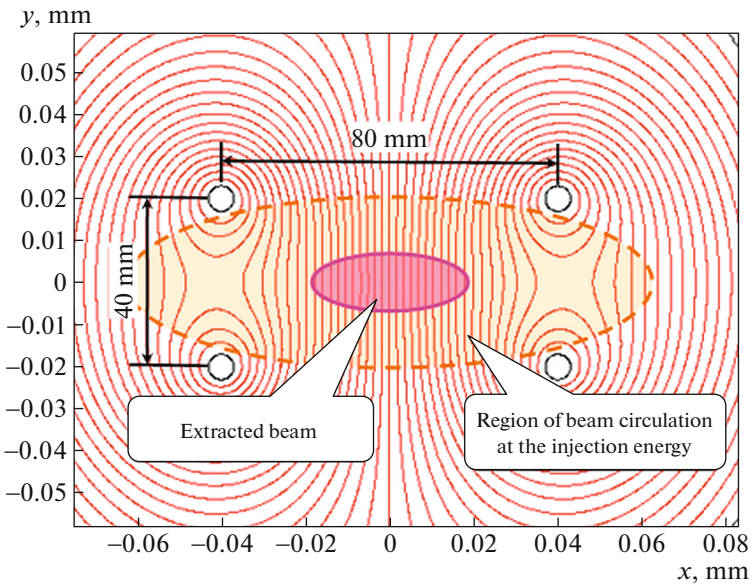

Fig. 1. Diagram of the formation of a magnetic field by current-carrying conductors.

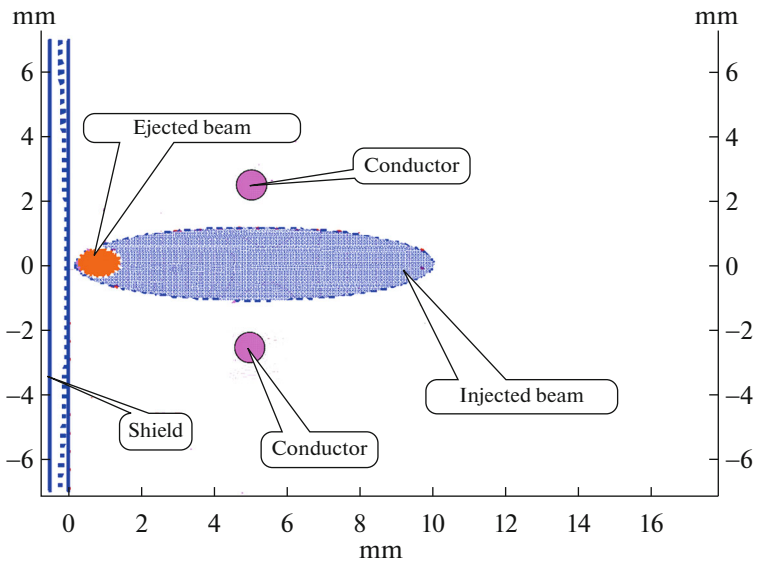

Fig. 2. Arrangement of the beams relative to the elements of the kicker magnet.

of ejection. It is under these conditions that the energy efficiency of the ironless magnet is comparable to the efficiency of traditional magnets or even exceeds it. At the same time, a sufficiently high uniformity of the magnetic field can be achieved in the working area.

1.2. Asymmetric Kicker Magnet

When the dimensions of extracted beams are significantly smaller than the chamber dimensions, a preliminary adiabatic displacement of the beam towards the extraction (the so-called bump) is commonly used in the extraction zone. This makes it possible to significantly lower the requirements for the integral of the kicker-magnet field. An asymmetric kicker-magnet design without a ferromagnetic core is applicable for such variants of the beam extraction since it consumes less energy for creating a field in the desired area of the accelerator aperture. The basic design of such a kicker magnet is shown in Fig. 2.

The magnetic field in the region of the extracted beam is formed by a pair of current-carrying conductors and a conductive shield. In the simplest case, the shield is flat.

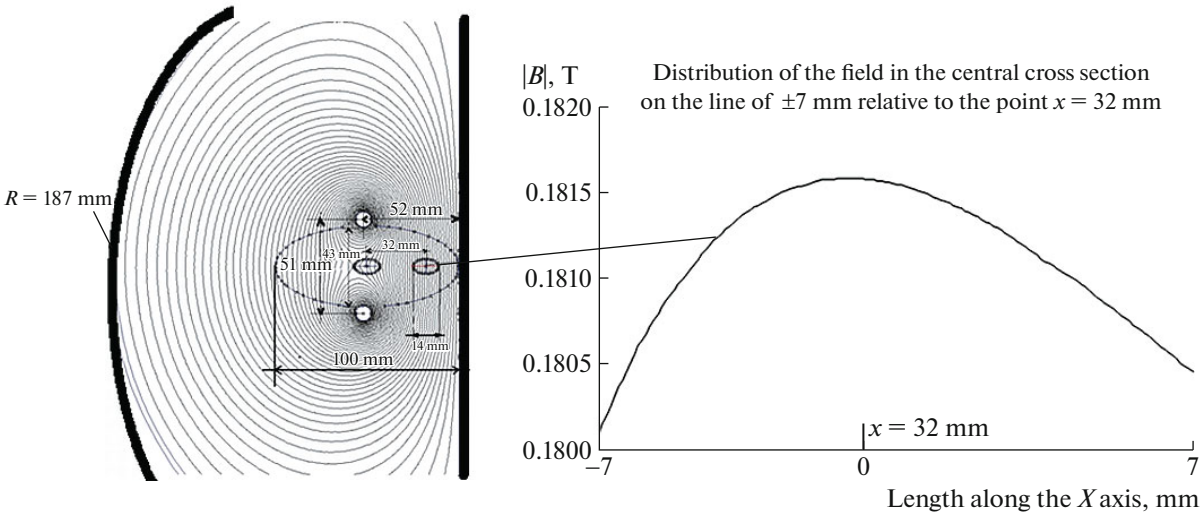

Fig. 3. 2D pattern of the field of the kicker magnet in its cross section and the uniformity of the field in the beam region.

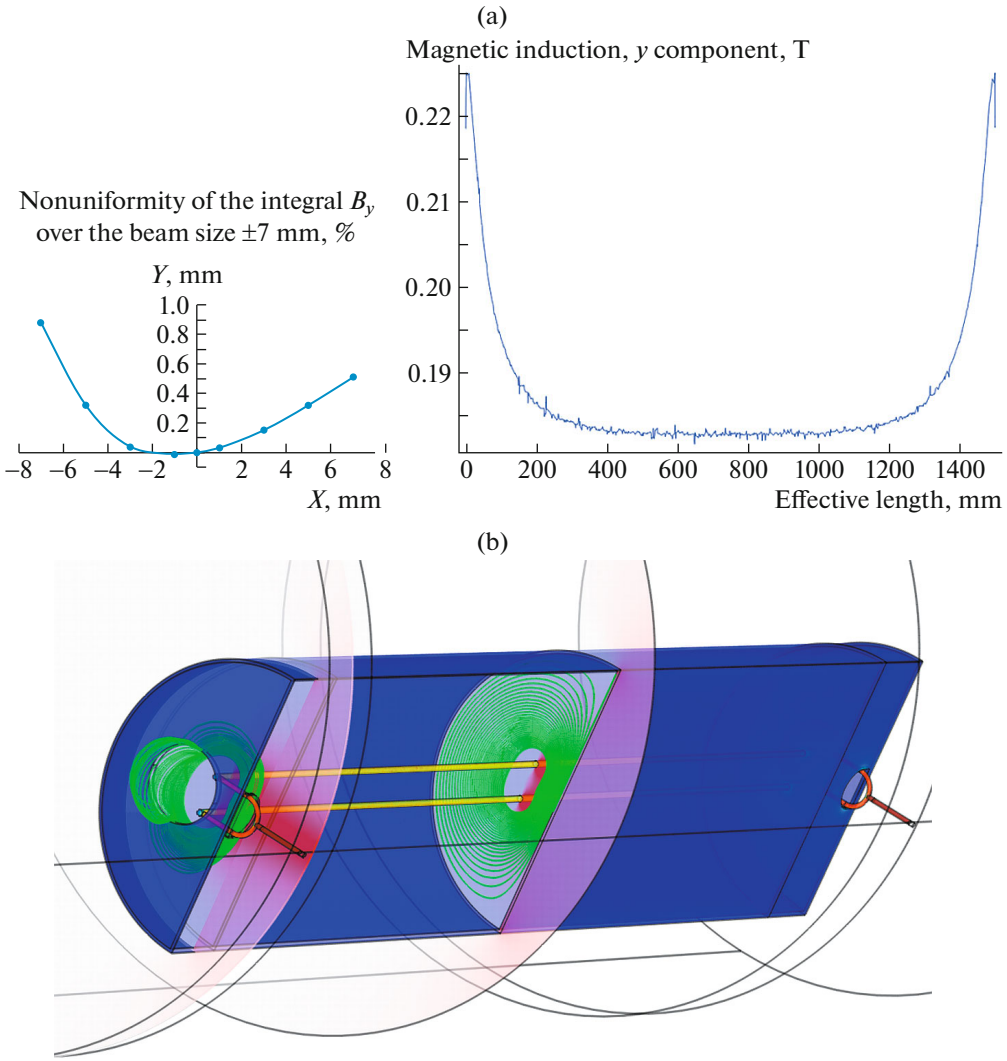

Fig. 4. (a) Computer 3D simulation of the kicker-magnet field: the nonuniformity of the transverse integral of the field and the distribution of the *y* component of the field along the effective length of the magnet, and (b) the structure of the force lines in two cross sections (at the center and at the entrance to the magnet).

2. MAIN PARAMETERS OF THE KICKER MAGNET FOR BEAM EXTRACTION FROM THE BOOSTER OF THE NICA COMPLEX

A kicker magnet was developed for the NICA accelerator complex (JINR, Dubna) [3] to eject ions into the beamline that connects the Booster and Nuclotron synchrotrons [4]. The kicker magnet does not have a ferromagnetic core; it consists of one pair of conductors connected in parallel and a steel shield with a semicircular section having a flat wall in the region of the extracted beam [5]. The wall replaces the second pair of conductors with the opposite direction of the current, which is symmetrical with respect to the beam center. The inductance of this design is 650 nH. The mutual geometry of the electrodes and the shield forms the necessary configuration of the magnetic field in the beam orbit with a uniformity of approximately 1.6% (Fig. 3). The main parameters of the kicker magnet are presented below:

Effective length, m	1.6
Maximum rigidity of extracted particles, T m	25
Maximum magnetic field, T	0.18
Maximum current in the electrodes, kA	32
Flat-top duration, ns	500
Duration of the pulse leading edge, ns	500
Diameter of working electrodes, mm	8

Different modes were simulated in order to optimize the power-supply circuit of the kicker magnet.

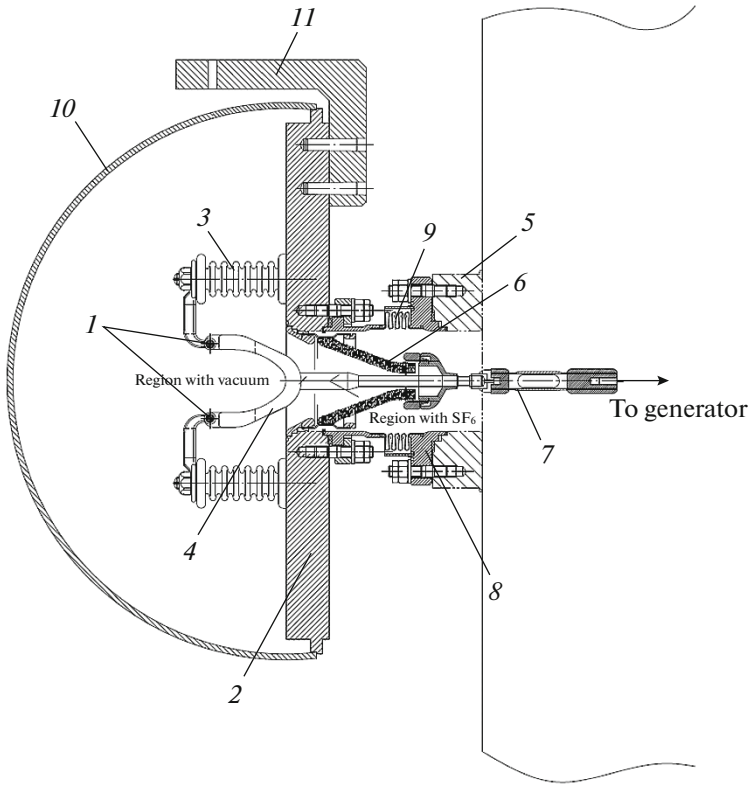

Fig. 5. Cross section of the kicker magnet at the site of the high-voltage bushing of the generator: (*1*) working electrodes, (*2*) shielding support wall (plate), (*3*) support insulators, (*4*) electrode holder, (*5*) flange of the generator housing, (*6*) feedthrough high-voltage insulator, (*7*) flexible conductive part of the current lead, (*8*) current-lead housing, (*9*) bellows isolation, (*10*) shield, and (*11*) geodesic bracket.

The selected power-supply circuit for a pair of electrodes with an inductance of 650 nH included two generators connected from the opposite ends with different polarity of the output pulse currents. This power-supply circuit has made it possible to reduce the effective inductance of the kicker magnet by two times and, as a result, to obtain the required pulse rise rate and flat-top duration at acceptable generator parameters.

Figure 4 shows the results of the simulation of the kicker-magnet field in a 3D model using the COMSOL package.

3. DESCRIPTION OF THE KICKER MAGNET DESIGN

The cross section of the magnet near the current lead is shown in Fig. 5; the main units are marked in the diagram.

The fast ion extraction from the Booster is performed in two stages. At the first stage, the circulating beam is guided to the plate (*2* in Fig. 5). At the second stage, the kicker magnet acts on the beam, and ions are actually extracted from the Booster.

Figure 6 shows photos both of the external appearance of the finished magnet with plugs protecting high-voltage current leads and of the inner vacuum chamber of the magnet with working electrodes.

High-voltage bushings (see Fig. 5) are a coaxial structure consisting of a sealed stainless-steel housing, flexible copper current lead *7* from the side of the entrance to the generator housing, a feedthrough high-voltage insulator *6* made of vacuum-tight ceramics with a 99.7% Al_2O_3 content, and electrode holder *4*. The bushings have a sulfur hexafluoride (SF_6) working medium at a pressure as high as 0.5 gauge atmosphere and allow transmission of pulses with an amplitude of up to 60 kV to the kicker electrodes. The electrode holder *4* makes it possible to compensate for possible thermal deformations of the structure during vacuum heating of the magnet and during mechanical vibrations of the electrodes when a high-voltage pulse is passed through them. The electrodes themselves with a holder of a certain shape are fixed in positions with necessary vertical and horizontal clearances in

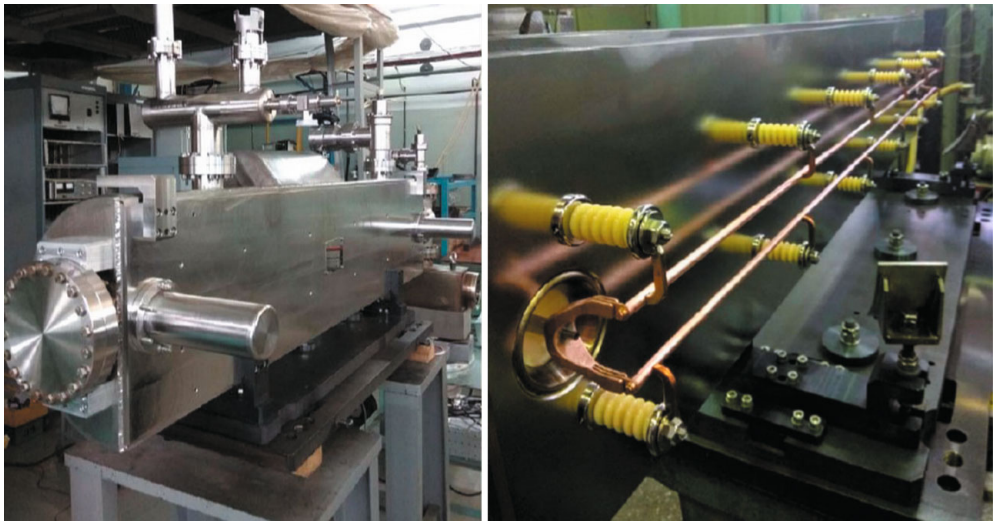

Fig. 6. Kicker magnet in the process of its production: a general view of the finished magnet with plugs protecting high-voltage current leads (on the left) and the inner vacuum part of the magnet with the working electrodes (on the right).

accordance with the size of the circulating-beam aperture; they do not impede its passage through the vacuum chamber. The electrodes are attached to the shielding plate by means of supporting ceramic insulators *3*. The number of insulators was optimized based on the calculations of the mechanical loads during the passage of working pulses.

Fig. 7. Generator part of the current lead with a flexible contact.

Figure 7 shows a part of the current lead from the side of the entrance to the generator housing. The flexible conductor *7* (see Fig. 5) consists of a copper braid with an internal nonconductive key used to maintain the volumetric shape of the conductor. This design allows precise connection of the magnet to the generators, eliminates possible mechanical loads of the insulator, and provides reliable electrical contacts. The kicker magnet itself is placed on a special stand and is positioned on the accelerator using special adjustment elements according to geodetic signs located on brackets *11* (see Fig. 5).

Computer simulation was carried out for the electrode part of the current lead (Fig. 8) in the electrostatic mode to identify particularly stressed places, and its results were taken into account when optimizing the design of the bushing body. The maximum field strengths of up to 90 kV/cm were obtained in the final

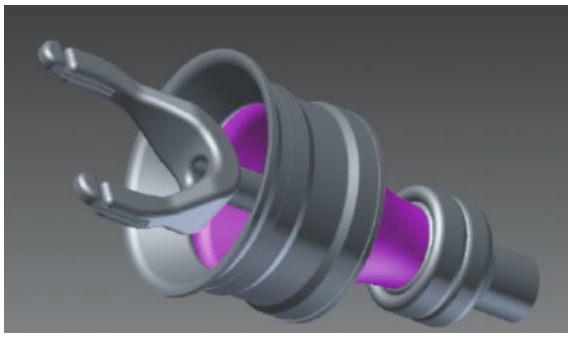

Fig. 8. Electrode part of the current lead.

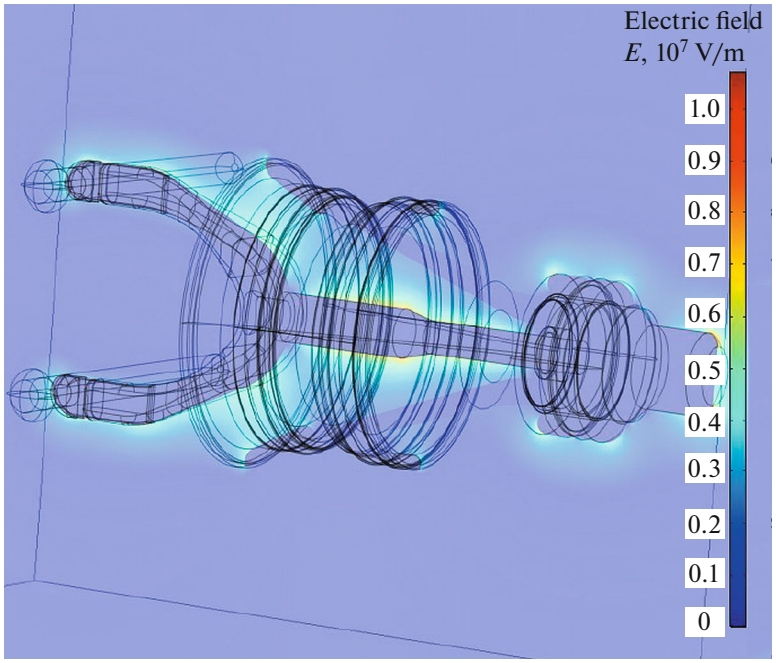

Fig. 9. Results of the simulation of the electric field strength.

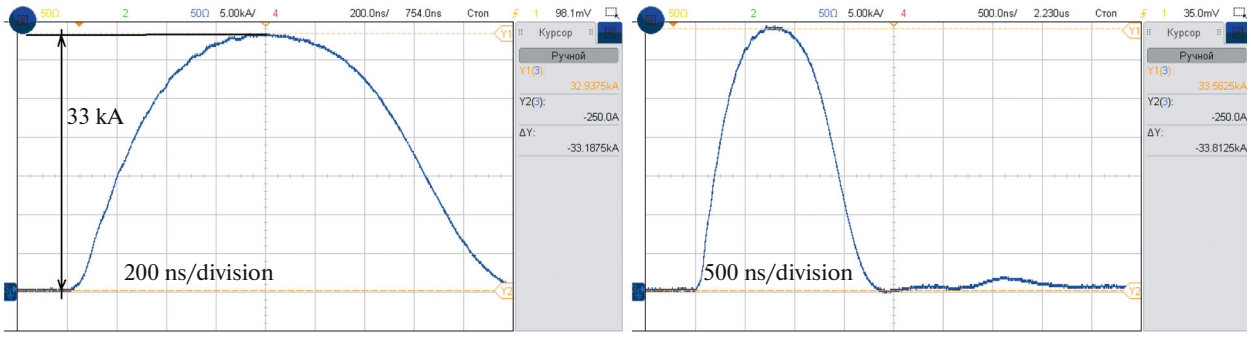

Fig. 10. Results of the tests of the kicker magnet generators into an equivalent load: the Rogowski loop signal at a charging voltage of 47 kV; the current amplitude was 33 kA.

version of the design both in ultrahigh vacuum and in the SF_6 atmosphere and were quite acceptable (Fig. 9).

4. RESULTS OF THE KICKER MAGNET TESTS

After the magnet was assembled, it was subjected to vacuum tests, during which a vacuum as high as 10^{-10} Torr was achieved. Electrical tests were also carried out at a constant voltage of up to 50 kV. Breakdowns in vacuum and in the bushings were not observed. Afterwards, the magnet was tested by applying pulses from the generators with the supply of SF_6 to the current leads.

Figure 10 shows the waveforms of the output generator pulses, which were picked off the Rogowski loops located in the generator part of the current lead.

The results of the magnet tests in the NICA complex at its workplace are shown in Fig. 11.

The He^{1+} and Fe^{14+} ions were successfully ejected into the Booster–Nuclotron beamline of the NICA complex with the calculated operating parameters of this kicker magnet. The ejection of iron ions was obtained in the mode of partial operating Booster

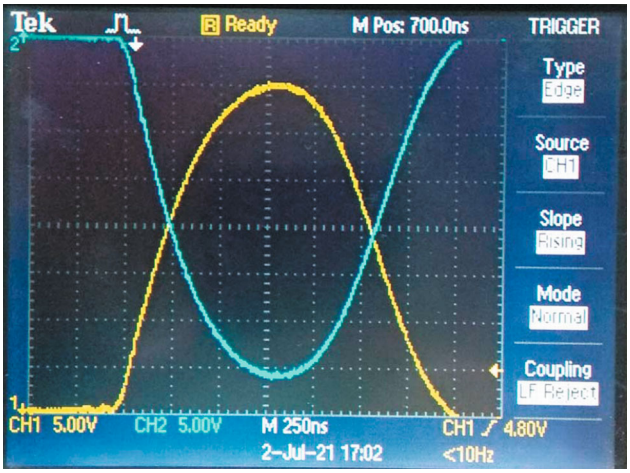

Fig. 11. Pulses picked off the Rogowski loops from "plus" and "minus" generators when running the kicker magnet in the Booster–Nuclotron beamline. The voltage was 45 kV, and the current amplitude was 32 kA.

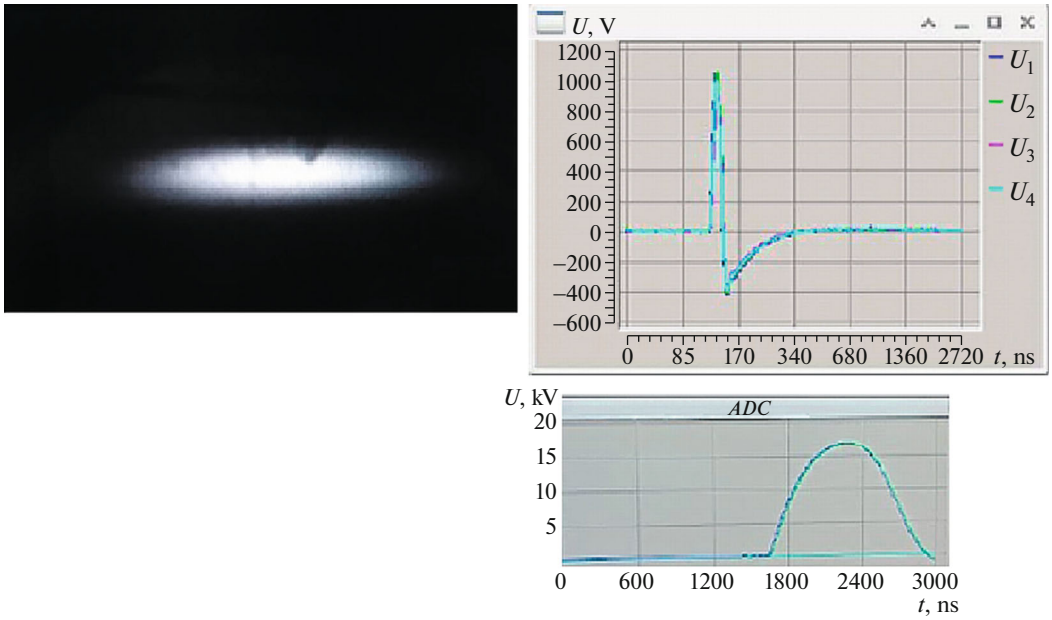

Fig. 12. Screenshot from the control panel: a beam ejected from the NICA Booster on a phosphor (on the left), the signals from the pickup electrodes when the beam was ejected from the Booster (at the top on the right), and kicker pulses (at the bottom on the right).

energy of up to 240 MeV/nucleon at a kicker magnet voltage as high as 17 kV and, hence, a current of 12 kA (Fig. 12), which corresponds to the maximum field in the magnets of the beamline for transporting non-stripped ions with $Z/A = 4$.

A maximum current of 32 kA and a voltage of 45 kV are needed for a full operating energy of the Booster, which is 600 MeV/nucleon for ions with $Z/A = 6$. During the Booster run, the kicker magnet was successfully trained and tested with these parameters over several hours without direct beam extraction.

CONFLICT OF INTEREST

The authors declare that they have no conflicts of interest.

REFERENCES

1. Shvedov, D.A., Anchugov, O.V., Kiselev, V.A., Korepanov, A.A., and Sinyatkin, S.V., *Instrum. Exp. Tech.,* 2015, vol. 58, no. 3, pp. 319–324. https://doi.org/10.1134/S0020441215030112
2. Alexandrov, V.S., Gorbachev, E.V., Tuzikov, A.V., and Fateev, A.A., *Phys. Part. Nucl. Lett.,* 2012, vol. 9, nos. 4–5, p. 425. https://doi.org/10.1134/S1547477112040073

3. Trubnikov, G., Agapov, N., Brovko, O., Butenko, A., Donets, E., Eliseev, A., Fimushkin, V., Gorbachev, E., Govorov, A., Ivanov, E., Karpinsky, V., Kekelidze, V., Khodzhibagiyan, H., Kovalenko, A., Kozlov, O., et al., *Proc. 4th Int. Particle Accelerator Conference IPAC'13,* Shanghai, 2013, p. 1343.

4. Tuzikov, A., Butenko, A., Donets, D., Govorov, A., Levterov, K., Meshkov, I., Smirnov, A., Syresin, E., Volkov, V., Zhuravlev, A., Kiselev, V., Okunev, I., Sinyatkin, S., and Tasset-Maye, O., *Proc. 26th Russian Particle Accelerator Conference (RuPAC-2018),* Protvino: Institute for High Energy Physics Named by A.A. Logunov of National Research Center "Kurchatov Institute," October 1–5, 2018, p. 52. https://doi.org/10.18429/JACoW-RUPAC2018-TUCDMH01

5. Aleksandrov, V., Fateev, A.A., and Tuzikov, A., *Proc. 25th Russian Particle Accelerator Conference RuPAC-2016,* St. Petersburg, 2016, p. 566. https://doi.org/10.18429/JACoW-RuPAC2016-THPSC013

Translated by N. Goryacheva